Report for exercise 4 from group C

Tasks addressed:	5
Authors:	Aleksi Kääriäinen (03795252) Danqing Chen (03766464) Julia Xu (03716599) Joseph Alterbaum (03724310)
Last compiled:	2024–09–27

The work on tasks was divided in the following way:

Aleksi Kääriäinen (03795252)	Task 1	25%
	Task 2	25%
	Task 3	25%
	Task 4	25%
	Task 5	25%
Danqing Chen (03766464)	Task 1	25%
	Task 2	25%
	Task 3	25%
	Task 4	25%
	Task 5	25%
Julia Xu (03716599)	Task 1	25%
	Task 2	25%
	Task 3	25%
	Task 4	25%
	Task 5	25%
Joseph Alterbaum (03724310)	Task 1	25%
	Task 2	25%
	Task 3	25%
	Task 4	25%
	Task 5	25%

Report on task 1, Vector fields, orbits, and visualization

1 Vector Fields, Orbits, and Visualization

In this task we had to produce phase portraits for different kinds of linear dynamical systems. As Kuznetsov showed in [2, p. 49], the topological classification of a linear dynamical system depends on its' eigenvalues' positions on the real-imaginary axis.

For this task, we used two different parameterized matrices as dynamical systems and plotted their phase portraits. The matrices are:

$$A_1 = \begin{bmatrix} \alpha & 1 \\ 1 & \alpha \end{bmatrix}, \text{ and}$$
$$A_2 = \begin{bmatrix} 0 & \alpha \\ -\alpha & -\alpha \end{bmatrix}.$$

The code used for producing the following plots can be found in `./task1.ipynb`.

Figure 1: Phase portraits

(a) Stable node

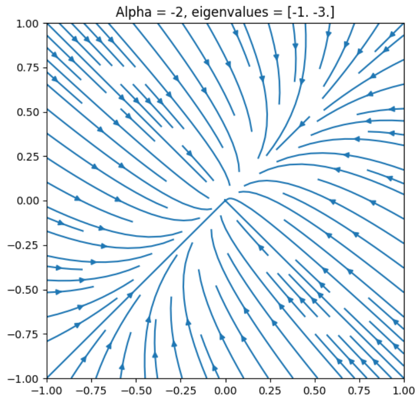

(b) Stable focus

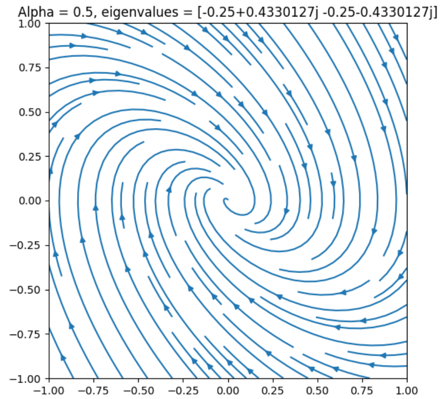

(c) Unstable node

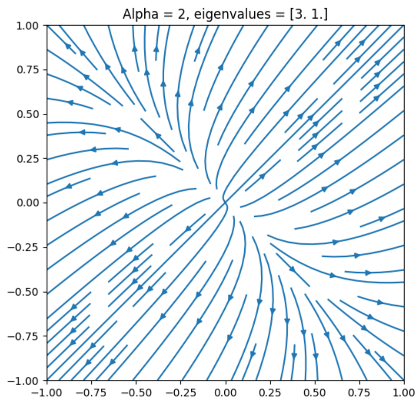

(d) Unstable focus

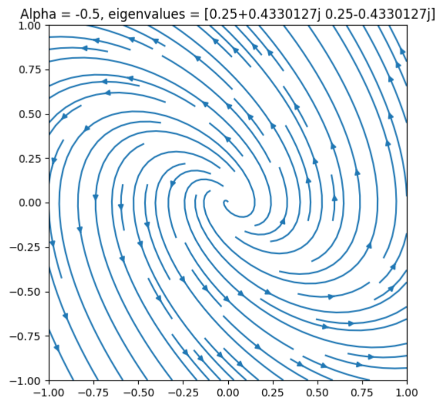

(e) Saddle

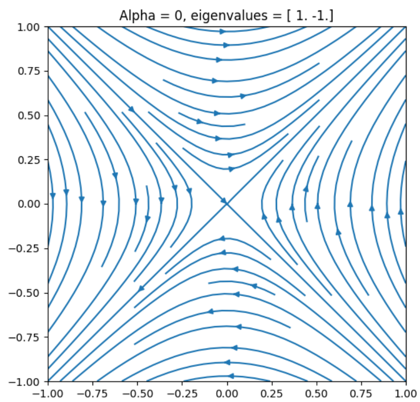

The figures 1a, 1c and 1e were produced with matrix A_1, while figures 1b and 1d were produced using matrix A_2 with the α values stated in the titles of the plots. The plots also include the eigenvalues of the used matrix in the title, to ensure that they correspond with the positions in the real-imaginary axis shown in [2, p. 49]. For example, a matrix with 2 real eigenvalues, where one is positive and the other negative is classified as a saddle.

Kuznetsov [2, p. 43] defines the topological equivalency among two dynamical systems as:

Definition 1. *A dynamical system $\{T, \mathbb{R}^n, \varphi^t\}$ is called locally topologically equivalent near an equilibrium x_0 to a dynamical system $\{T, \mathbb{R}^n, \psi^t\}$ near an equilibrium y_0 if there exists a homeomorphism $h : \mathbb{R}^n \implies \mathbb{R}^n$ that is*

1. *defined in a small neighbourhood $U \subset \mathbb{R}^n$ of x_0*
2. *satisfies $y_0 = h(x_0)$*
3. *maps orbits of the first system in U onto orbits of the second system in $V = h(U) \subset \mathbb{R}^n$, preserving the direction of time.*

Kuznetsov [2, p. 48] also states that nodes and foci of the same stability are topologically equivalent. This implies that the systems 1a and 1b are topologically equivalent, and so are systems 1c and 1d. Indeed, if one were to 'twist' 1a in the origin clockwise, they would reach a similar state to 1b. the twist homeomorphism is also reversible, and preserves the direction of time, fulfilling all requirements for topological equivalency in the definition. The same holds for 1c and 1d.

Report on task 2, Common bifurcations in nonlinear systems

2 Common bifurcations in nonlinear systems

2.1 Bifurcation of a dynamical system

In this task, we studied two different dynamical systems on the real line, namely

$$\dot{x} = \alpha - x^2 \tag{1}$$
$$\dot{x} = \alpha - 2x^2 - 3 \tag{2}$$

The systems' steady states can be found when setting $\dot{x} = 0$. Thus, for system 1, the steady states are:

$$\begin{aligned} 0 &= \alpha - x^2 \\ x &= \pm\sqrt{\alpha}, \end{aligned}$$

and for system 2:

$$\begin{aligned} 0 &= \alpha - 2x^2 - 3 \\ 2x^2 &= \alpha - 3 \\ x &= \pm\sqrt{\frac{\alpha - 3}{2}}. \end{aligned}$$

As α increases through zero, system 1 transitions from having no steady states (for $\alpha < 0$), to having one steady state at $x = 0$ (for $\alpha = 0$), to having two steady states $x = \pm\sqrt{\alpha}$ (for $\alpha > 0$). The bifurcation happening at $\alpha = 0$ is thus a saddle-node bifurcation.

2.2 Bifurcation graphs of the two systems

Figure 2: Bifurcation graphs

(a) system 1 (b) system 2

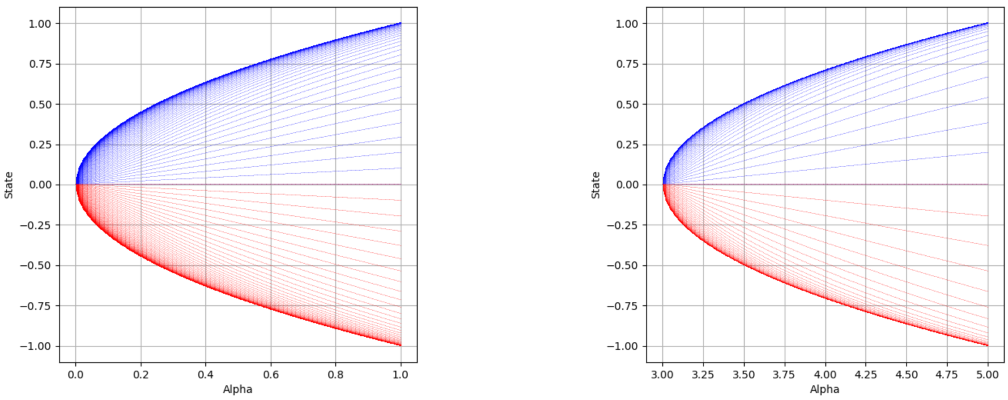

The implementation for Task 2 can be found in `./task2.ipynb` and the results are visualised in Figure 2 showing the bifurcation graphs for both of the systems. The blue points show the evolution of the system over time starting from initial state $x_0 = 0$ for a given α. The evolution of the system is thus visible in the y-direction of the graph, and was calculated with Scipy's `solve_ivp` function. The plot also shows the two systems' steady states as a function of α. The blue curve shows the stable steady states of a system, whereas the red curve shows the unstable steady states of a system. For both plots, the saddle-node bifurcation point is also visible, although unmarked. For system 1 the saddle-node bifurcation point is at $\alpha = 0$, as stated previously. For system 2, the saddle-node bifurcation point is at $\alpha = 3$.

2.3 Topological equivalency of the two systems

To determine whether two systems are topologically equivalent, the first requirement is that they have the same number of steady states. Thus the two systems can't be topologically equivalent at $\alpha = 1$, since system 1 has 2 steady states and system 2 has 0 steady states at $\alpha = 1$.

Let us take a closer look at the systems at $\alpha = -1$. System 1 takes the form:

$$\dot{x} = -1 - x^2,$$

while system 2 takes the form:

$$\begin{aligned}\dot{x} &= -1 - 2x^2 - 3 \\ &= -4 - 2x^2\end{aligned}$$

For the systems to be topologically equivalent, they have to be qualitatively the same, i.e. they must behave the same way. Neither system have steady states at $\alpha = -1$. Both systems are always negative and decreasing, i.e. $x \to -\infty$ as $t \to \infty$, meaning their behavior is similar. These facts about the two systems make us confident that there exists a 1-to-1 mapping between the two systems, meaning that the two systems are topologically equivalent at $\alpha = -1$. And if the two systems are topologically equivalent, they by definition have to have the same normal form.

Report on task 3, Bifurcations in higher dimensions

3 Bifurcations in higher dimensions

This task consists of two parts where firstly phase diagrams and orbits of an Andronov-Hopf bifurcation are plotted. Then, in the second part, the cusp bifurcation is visualized in a 3D plot. The notebook `task3.ipynb` is structured into its respective task parts and thoroughly documented.

3.1 Andronov-Hopf Bifurcation

The Andronov-Hopf bifurcation is a bifurcation for systems with one parameter and two-dimensional state spaces. Its vector field in normal form is given by:

$$\dot{x}_1 = \alpha x_1 - x_2 - x_1(x_1^2 + x_2) \tag{3}$$

$$\dot{x}_2 = x_1 + \alpha x_2 - x_2(x_1^2 + x_2) \tag{4}$$

3.1.1 Three Phase Diagrams

In figure 3, three phase diagrams at representative values of α ($\alpha = [-0.5, 0, 0.5]$ are plotted to visualize the bifurcation.

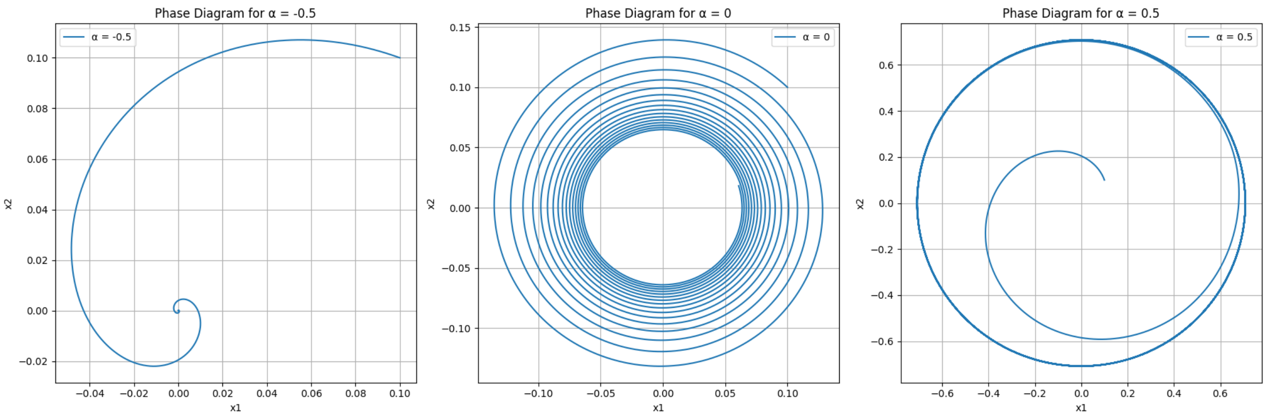

Figure 3: Phase diagrams of Andronov-Hopf bifurcation (one parameter)

3.1.2 Visualization of Two Orbits through Numerical Solver

In figure 4, two orbits are shown that track the system forward in time with starting points at (2,0) and (0.5,0) and $\alpha = 1$. For each starting point `solve_ivp()` is called to solve the dynamical system.

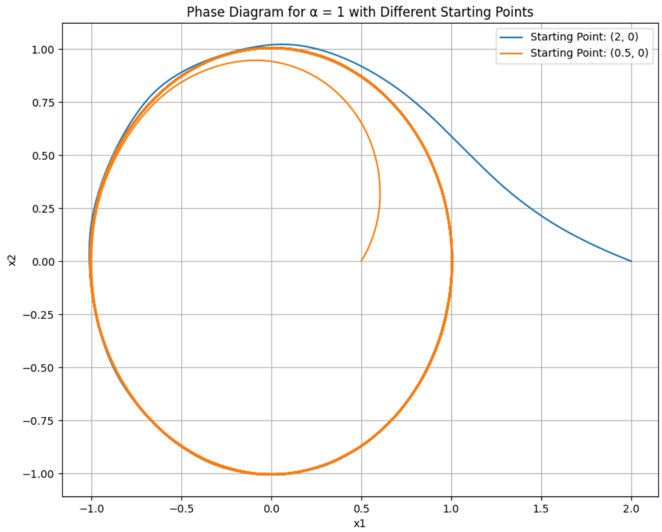

Figure 4: Two orbits of the system forward in time, $\alpha = 1$

3.2 Visualization of Cusp Bifurcation

This part of the task visualizes a different bifurcation in a three-dimensional plot. The function `plot_3d_surface()` in `utils.py` is used to achieve this.

Cusp bifurcation already occurs in an one-dimensional state space $X = \mathbb{R}$ and deals with two instead of just one parameter. The normal form of cusp bifurcation is

$$\dot{x} = \alpha_1 + \alpha_2 x - x \tag{5}$$

Figure 5 shows the plotted 3D cusp bifurcation diagrams in various angles.

Figure 5: 3D plot of cusp bifurcation in different viewing angles

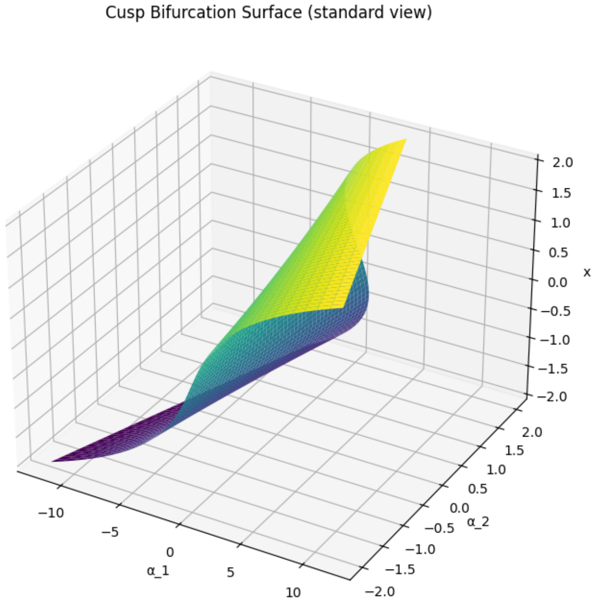

(a) Standard view

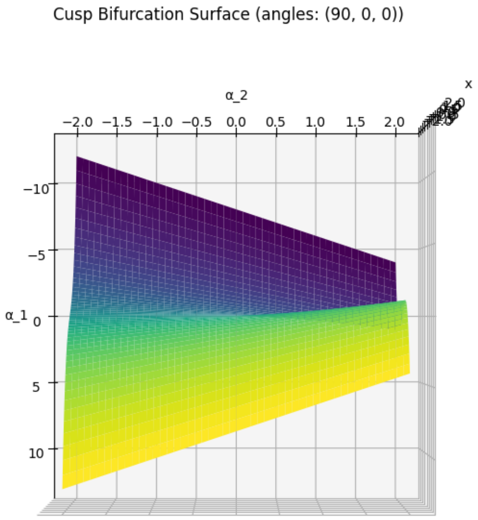

(b) Rotation around x-axis to get top view

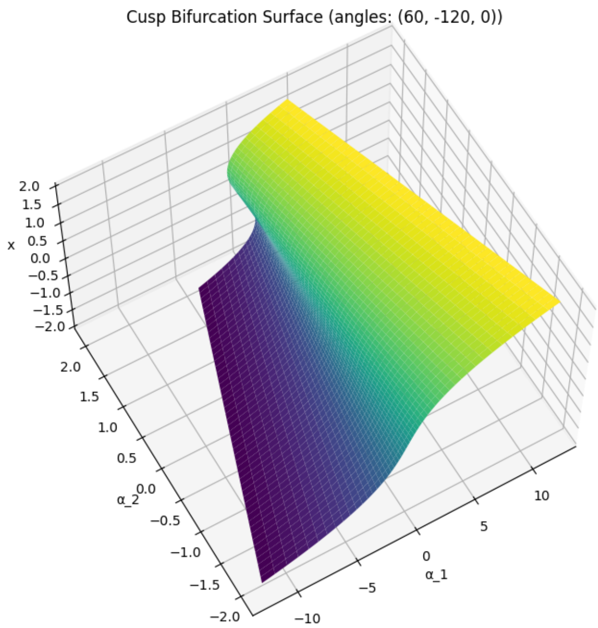

(c) Rotation around x- and y-axis to get angled top view

To explain why this bifurcation is called *cusp bifurcation* a definition for *cusp* is needed: A cusp (in dynamical systems) refers to a point where a system's trajectory changes direction sharply. This can be clearly seen in figure 5b and 5c around the points $\alpha_1 = 0$ and $\alpha_2 = 2.0$ where the x-value suddenly changes from a low value (blue) to a high number (green) (seen from bottom to top along the x-axis).

Report on task 4, Chaotic dynamics

4 Dynamical Systems Analysis

Dynamical systems can behave in very irregular ways, and changes in their parameters can lead to very drastic changes in their behavior.

Consider the discrete map

$$x_{n+1} = rx_n(1 - x_n), \quad n \in \mathbb{N},$$

with the parameter $r \in (0, 4]$ and $x \in [0, 1]$. Perform the following bifurcation analyses separately:

4.1 Part 1 – Analyze the behavior of the map as the parameter r varies from 0 to 2

4.1.1 $r \in (0, 2)$

- Which bifurcations occur?
- At which numerical values do you find steady states of the system?

Setup

As the parameter r varies, the logistic map exhibits a range of behaviors from stable fixed points to periodic oscillations and chaos. The bifurcation diagram is a visual summary of how the fixed points (or periodic orbits) of the system change as r is varied. We implement the logistic map and generate its bifurcation diagram for $r \in [0, 2]$. .

The result of the visualization can be found in 6

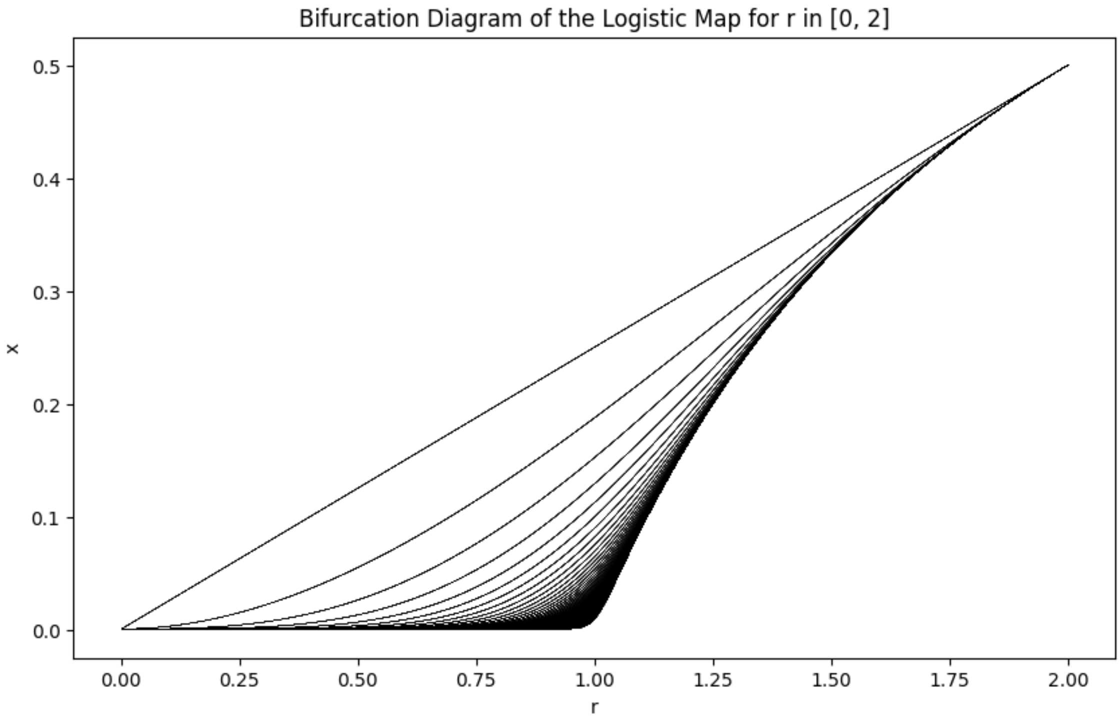

Figure 6

For $r \in (0, 1)$:

- The fixed point $x^* = 0$ is stable.
- The trajectories converge to $x = 0$.

At $r = 1$:

- A bifurcation occurs.
- The fixed point $x^* = 0$ becomes unstable.

For $r \in (1, 2)$:

- The fixed point $x^* = 1 - \frac{1}{r}$ is stable.
- The trajectories converge to $x = 1 - \frac{1}{r}$.
- As r increases within this range, the fixed point moves closer to $x = 0.5$.

The bifurcation diagram shows the transition from stability at $x = 0$ to the new stable fixed point $x = 1 - \frac{1}{r}$ as r passes through 1. This behavior is characteristic of the logistic map and helps to illustrate how small changes in the parameter r can lead to significant changes in the system's dynamics.

4.1.2 $r \in [2, 4]$

Now vary r from 2 to 4.

- What happens?
- Describe the behavior (no formal proofs or exact statements necessary).

Plot a bifurcation diagram for r between 0 and 4 (horizontal axis), x between 0 and 1 (vertical axis), roughly indicating the positions of steady states and limit cycles. The result of the visualization can be found in 7

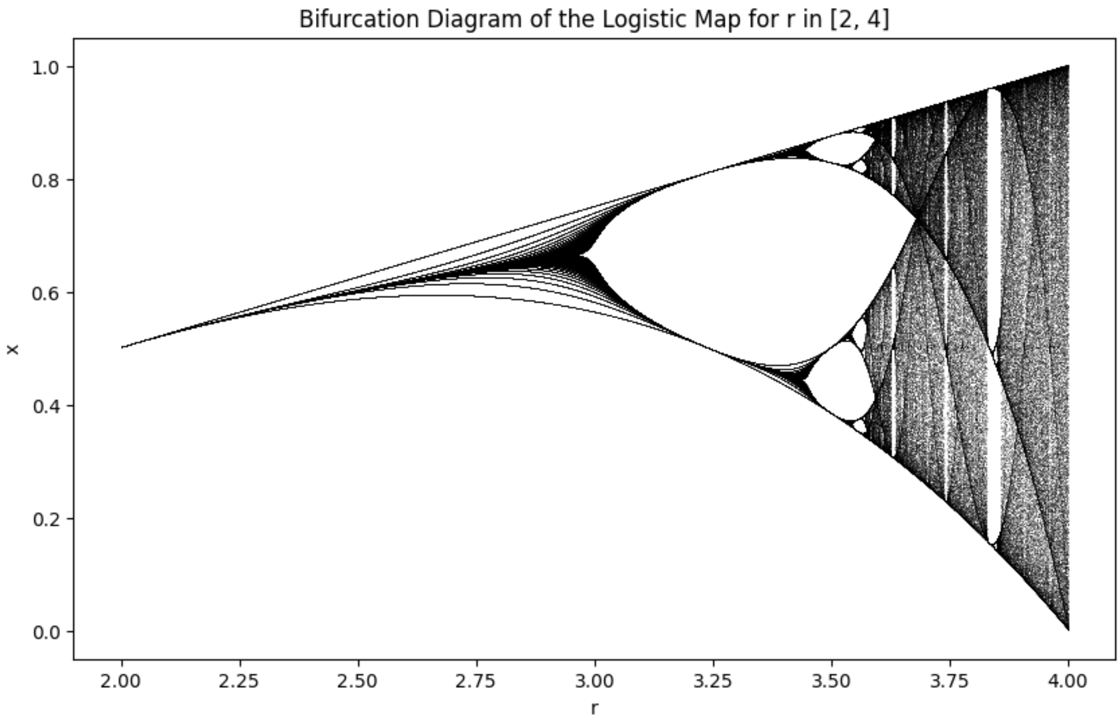

Figure 7

For $2 < r < 3$:

- **Period Doubling**: Starting at $r \approx 2$, the system initially exhibits a stable period-2 cycle. As r increases, each periodic orbit doubles, leading to period-4, period-8, and so on. This is known as period-doubling bifurcation.

- **Chaotic Onset**: Around $r \approx 3$, the system transitions to chaotic behavior. This is indicated by the dense, intertwined lines in the diagram, where the values of x do not settle into any periodic orbit but instead appear random.

For $r \approx 3.57$:

- **Full Chaos**: Near $r \approx 3.57$, the system fully enters a chaotic regime. The values of x are highly sensitive to initial conditions, and small changes can lead to vastly different trajectories. This region is characterized by the spread-out and seemingly random distribution of points.

For $3 < r < 4$:

- **Periodic Windows**: Within the chaotic region, there are intervals where the system temporarily returns to periodic behavior. These are visible as isolated islands or bands where the points converge to stable periodic cycles. For instance, at certain values of r, you can see period-3, period-5 cycles, etc.
- **Intermittency**: These periodic windows are interspersed with chaotic behavior, indicating that the system can switch back and forth between chaos and periodicity.

For $r \approx 4$:

- **High Chaos**: As r approaches 4, the system remains predominantly chaotic. This is evident from the dense and intricate patterns covering almost the entire range of x values. The system explores a wide range of states in an apparently unpredictable manner.

Key Observations

- **Period Doubling Route to Chaos**: The transition from simple periodic behavior to chaos through successive period-doubling is a hallmark of deterministic chaos in dynamical systems.
- **Chaotic Dynamics**: The system's behavior becomes unpredictable and highly sensitive to initial conditions in the chaotic regime, which is reflected in the broad spread of x values.
- **Periodic Windows**: Despite the overall chaotic nature, there are pockets of periodic behavior within the chaotic regions, showing the complex interplay between order and disorder in the system.

4.1.3 Full interval

Plot a bifurcation diagram for r between 0 and 4 (horizontal axis), x between 0 and 1 (vertical axis), roughly indicating the positions of steady states and limit cycles. The result of the visualization can be found in 8

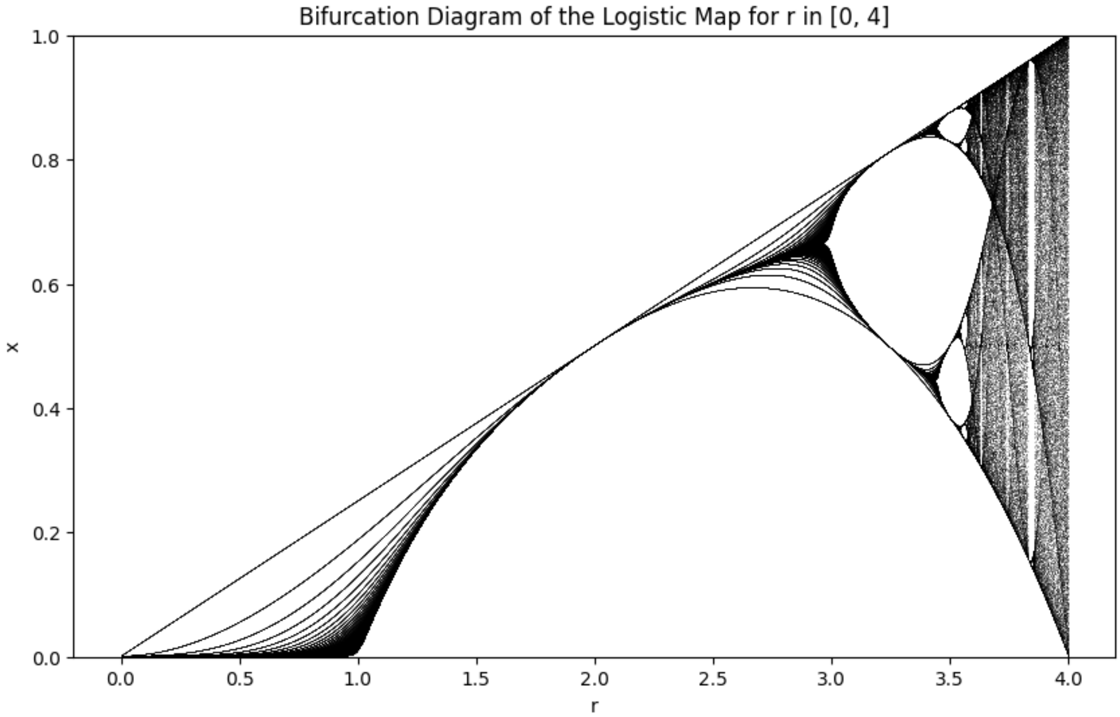

Figure 8

- $0 < r < 1$: Single stable fixed point.
- $r = 1$: Bifurcation where $x = 0$ becomes unstable.
- $1 < r < 3$: Successive period-doubling bifurcations leading to increasingly complex periodic cycles.
- $r \approx 3.57$: Onset of chaos with highly sensitive and seemingly random behavior.
- $3.6 < r < 4$: Periodic windows within the chaotic regime.
- $r \approx 4$: Fully developed chaos with dense, intricate patterns.

4.2 Part 2 – Application of Lorenz attractor

Dynamical systems in continuous time cannot have smooth evolution operators that produce chaotic dynamics if the dimension of the state space is smaller than three. The Lorenz attractor is a famous example of a system in three-dimensional space that forms a strange attractor, a fractal set on which the dynamics are chaotic.

Visualize a single trajectory of the Lorenz system starting at $\mathbf{x_0} = (10, 10, 10)$, until you reach the end time of $T_{\text{end}} = 1000$ (note that T_{end} is not the iteration count, but the simulated time!), at the parameter values $\sigma = 10$, $\beta = \frac{8}{3}$, and $\rho = 28$.

- What does the attractor look like?
- The chaotic nature of the system implies that small perturbations in the initial condition will grow larger at an exponential rate, until the error is as large as the diameter of the attractor.

Test this by plotting another trajectory from $\hat{\mathbf{x_0}} = (10+10^{-8}, 10, 10)$ in 3D, and separately plot the difference between the two trajectories over time (plot $\|\mathbf{x}(t)-\hat{\mathbf{x}}(t)\|_2$ against t, where $\mathbf{x}(t), \hat{\mathbf{x}}(t) \in \mathbb{R}^3$ are the two trajectories for the two initial conditions).

- At what time is the difference between the points on the trajectory larger than 1?

The result of the visualization can be found in 9, 10 & 11.

The first plot 9 depicts the trajectory of the Lorenz system starting from the initial conditions $(10, 10, 10)$ with $\rho = 28$. This trajectory illustrates the famous Lorenz attractor, which is characterized by its distinctive butterfly or figure-eight shape. The system quickly evolves from the initial conditions and starts to exhibit chaotic behavior, where the trajectory oscillates around two lobes of the attractor.

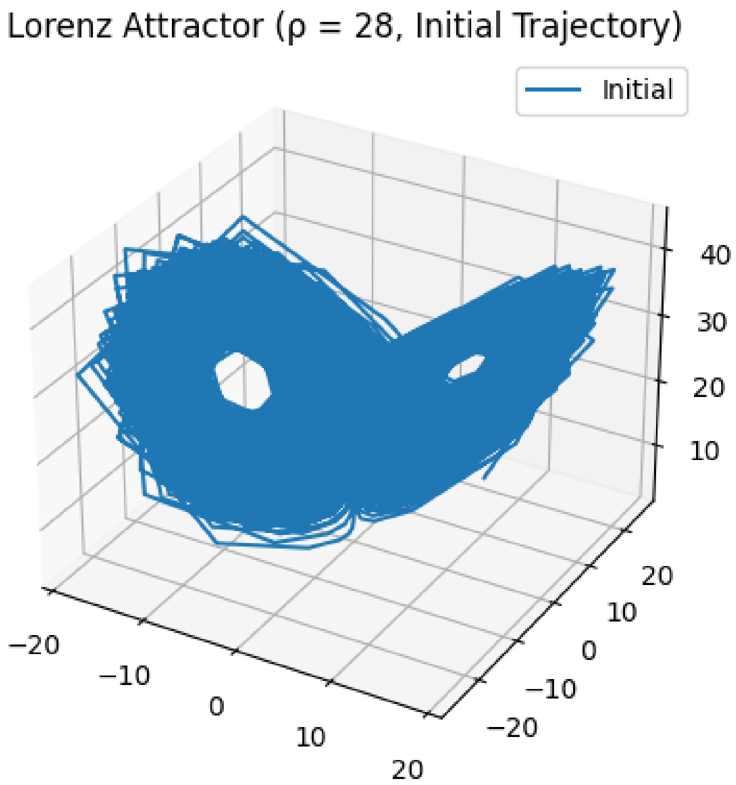

Figure 9

The second plot again shows the Lorenz attractor for $\rho = 28$. Here, the blue curve represents the trajectory starting from $\mathbf{x_0} = (10, 10, 10)$, and the orange curve represents the trajectory starting from $\hat{\mathbf{x_0}} = (10 + 10^{-8}, 10, 10)$. The trajectories quickly diverge, illustrating the chaotic nature of the system.

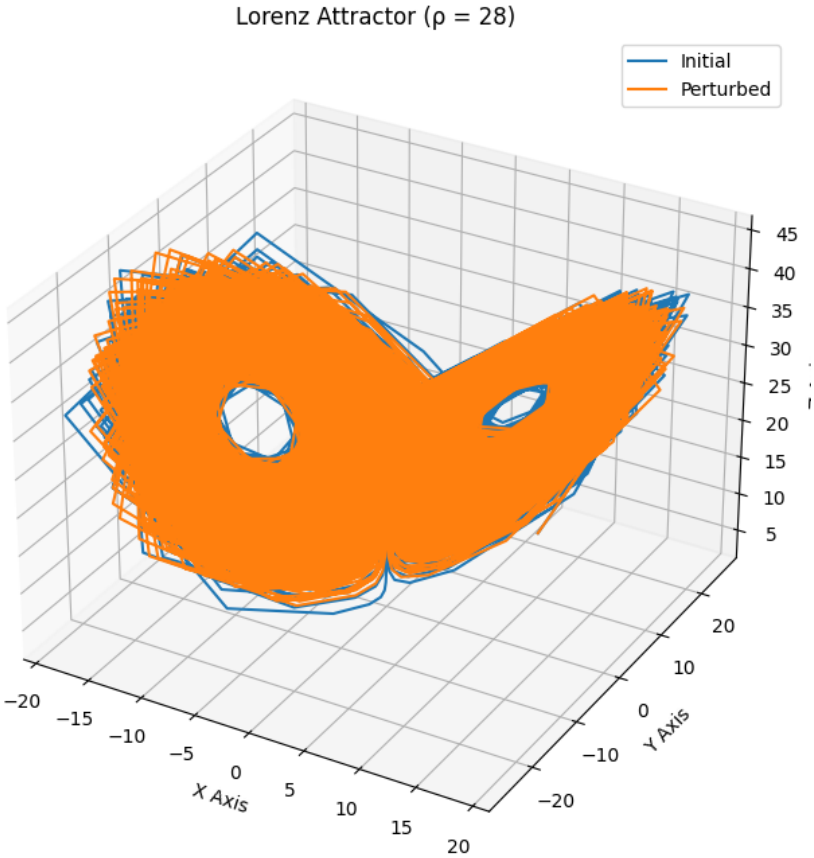

Figure 10

The third plot 11 shows the difference between the two trajectories over time, plotted on a logarithmic scale. The difference grows exponentially, which is characteristic of chaotic systems. Through our calculation we get that The difference between the trajectories is larger than 1 at time t = 24.90 for $\rho = 28$

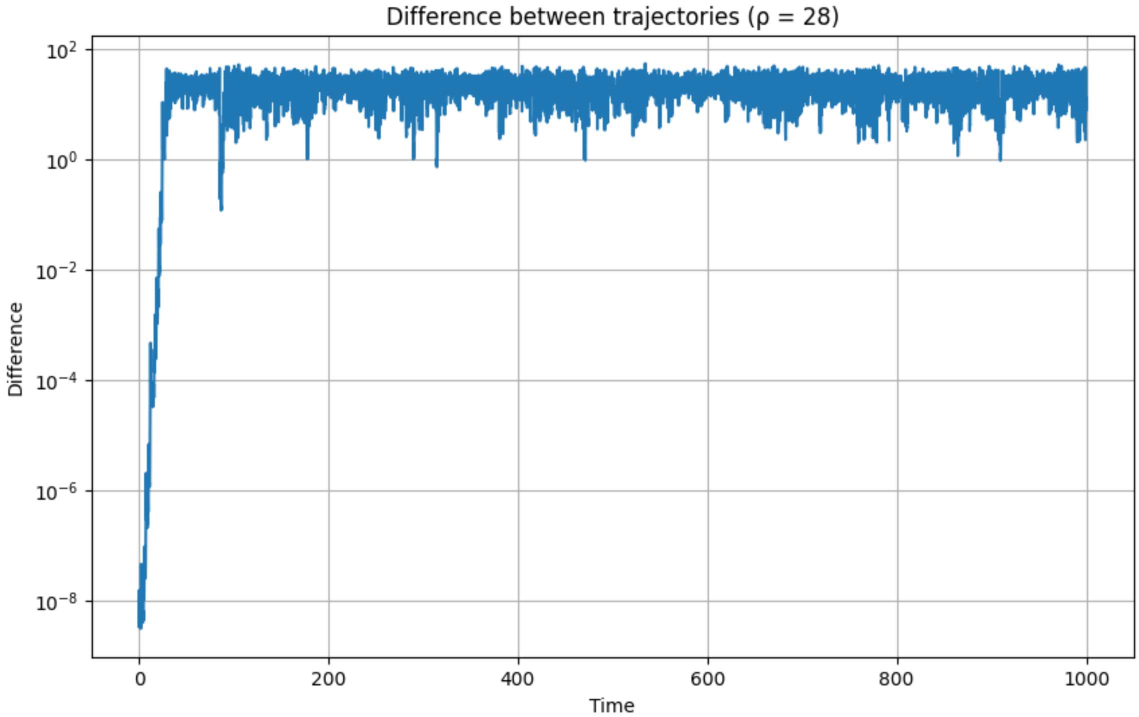

Figure 11

Now, change the parameter ρ to the value 0.5 and again compute and plot the two trajectories. What is the difference in terms of the sensitivity to the initial conditions? Is there a bifurcation (or multiple ones) between the value 0.5 and 28? Why, or why not?

The visualization can be found in 12 & 13.

The first plot shows the Lorenz system for $\rho = 0.5$. Unlike the case with $\rho = 28$, the trajectories do not diverge significantly, indicating non-chaotic behavior. Furthermore, they fully overlap in the plot.

The second plot shows the difference between the two trajectories over time, plotted on a logarithmic scale. The difference remains extremely small, indicating that the system is not sensitive to initial conditions for $\rho = 0.5$.

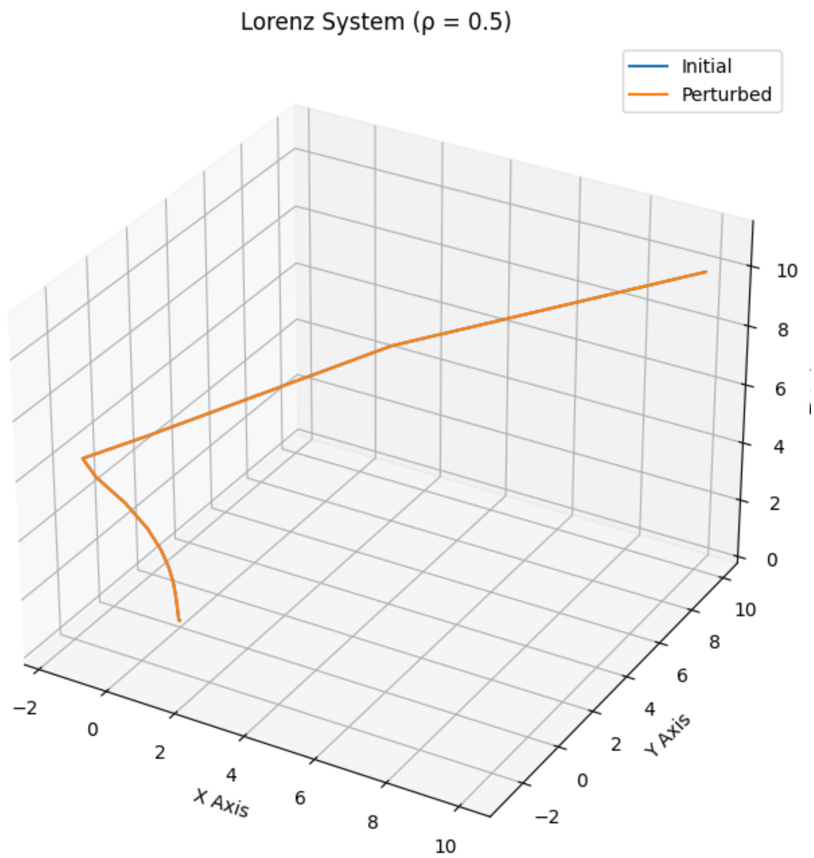

Figure 12

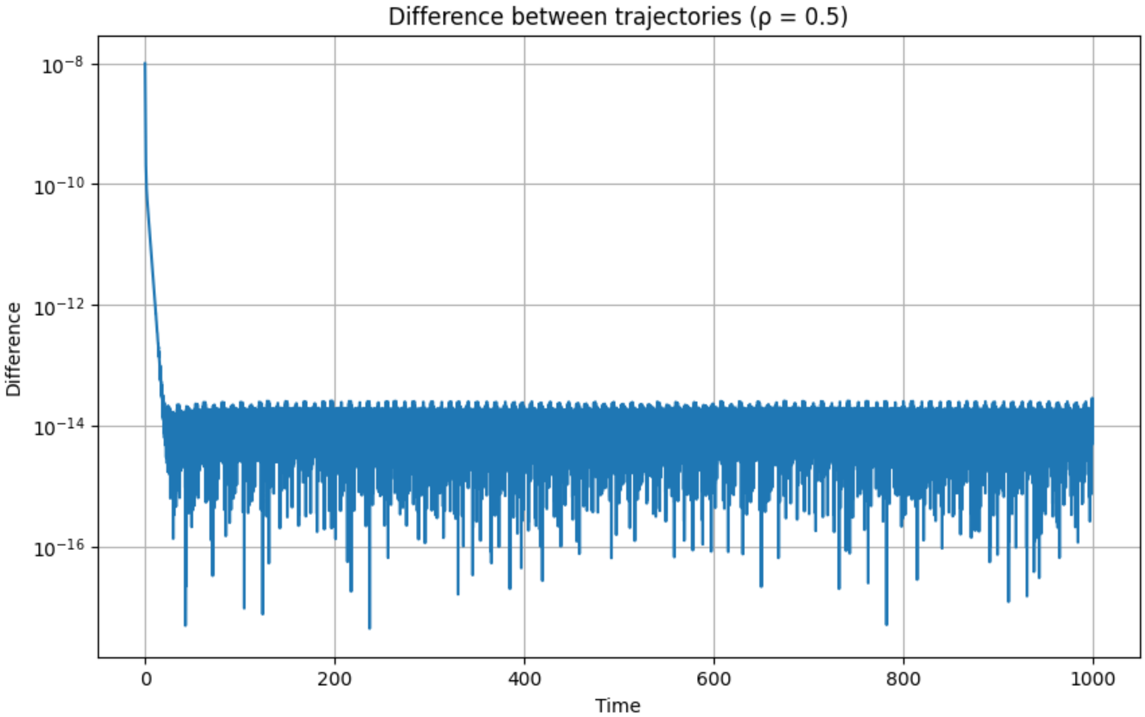

Figure 13

Key Observation

- For $\rho = 0.5$, the Lorenz system does not exhibit chaotic behavior. The trajectories of the initial and perturbed conditions remain close to each other.
- The difference between the trajectories stays very small over time, which is characteristic of stable, non-chaotic systems.
- Comparing the results for $\rho = 0.5$ and $\rho = 28$, we observe a bifurcation where the system transitions from non-chaotic to chaotic behavior. This suggests a bifurcation point between these values of ρ, where the dynamics of the system change significantly.

Through our calculation we got that the difference between the trajectories never exceeds 1 for $\rho = 0.5$.

Report on task 5, Bifurcations in crowd dynamics

5 Bifurcations in an SIR-model

5.1 Setup & Implementation of the SIR-model

The implementation of the SIR-model & simulations of specific configurations is divided into the JuPyter-notebook "*task5.ipynb*" and the module-file "*sir_model.py*". The actual behaviour of the model is specified in the module-file. Here, the function "*model*" realises the differential equations describing the SIR-model, namely one for each dimension of the state space – the number of susceptible S, infective I & recovered individuals R. For the specific equations we refer to the function or the paper by Shan & Zhu [1].
Another characteristic of this SIR-model is the dynamic modeling of the recovery rate μ depending on the number of hospital beds b. This feature is implemented in the function "*mu*" and computes the recovery rate μ based on parameters such as the number of infective individuals I & the number of hospital beds b. Again, for the specific formula and an explanation of the modeling approach we refer to Shan et. al. [1].
The Jupyter-notebook "*task5.ipynb*" uses the SIR-model implementation to simulate the behaviour of specific configurations. While specific information can be found in the notebook itself, the general pipeline is the following: First, the meta-parameters (time, tolerances, etc.) & model parameters (A, d, ν, etc.) are specified. Subsequently, an initial state is either sampled or given and the system of differential equations is solved with an initial value problem solver like Runge-Kutta or Adams/BDF, e.g., from the SciPy-package "*solve_ivp*". Afterwards, the solution can be visualised in different ways.
Apart from the two functions realising the SIR-model itself, two utility methods are given to compute parameters helping with the characterisation of the dynamic behaviour. Firstly, the function "*R0*" computes the reproduction number that is for example used to characterise equilibriums in the system, cp. Chap. 3 in [1]. Moreover, the indicator function "*h*" becomes important when looking at the existence & specific I-value of Hopf-bifurcations in the system.

5.2 First observations of the SIR-model behaviour

In the first part of the Jupyter-notebook "*task5.ipynb*" a first feeling for the SIR-model behaviour & the influence of the number of hospital beds b can be obtained. Therefore, the state space dimensions S, I & R are plotted separately over the time t and the relation between the recovery rate μ & number of infective individuals I is shown in a shared plot over time. The indicator function $h(I)$ shows the roots of the function characterising Hopf-bifurcation in the system, so in combination with chapter 4.2 of the paper by Shan & Zhu [1] a deeper understanding of the relation between endemic equilibria E_1 & E_2 and the occurence of Hopf-bifurcation can be gained. Further descriptions can be found in the Jupyter-notebook in Part 1.

5.3 Bifurcation with parameter b (number of hospital beds)

The second part of the Jupyter-notebook "*task5.ipynb*" concerns the task of observing the system behaviour from three different initial states under a varying number of hospital beds b. While we initially used 1000 values in the range from t = 1 to t = 15000, we later decided on a larger and more detailed time-grid from 1 to 150000. These meta-parameters of the simulation can be specified in the first few rows of the second part of the notebook.

5.3.1 Initial state 1 – (195.3, 0.052, 4.4)

The behaviour of the first initial state can be seen in Fig. 14a–14c. For values of $b \in [0.01, 0.0221)$ the system **converges** into a **stable fixed point** which is most likely one of the endemic equilibria (I & R non-zero), described in chapter 3 of the paper [1]. With rising b the time to convergence rises as well or equivalently spoken the system does more circles before converging into the fixed point in the centre. The corresponding trajectory is depicted in Fig. 14a and for $b > 0.021$ the time before convergence/number of circles grows rapidly. At $b = 0.022$ the system is still converging to a stable focus, as seen in Fig. 14b, but non-linearly becuase the rate of convergence is no longer exponential which is evident due to the large number of cycles before convergence. For this reason, $b = 0.022$ is characterised as the **bifurcation point** for this initial state.

Subsequently, for $b \in [0.0221, 0.023)$ the behaviour changes and a **stable limit cycle** appears instead of convergence to a fixed point. As seen in Fig. 14c for $b = 0.0225$, the system starts at the initial state and moves outwards into the limit cycle of an oval shape. One observation in comparison to before is the stretching of the limit cycle towards the disease-free equilibrium E_0 at the lower right side of the plot.

When adjusting b to even higher values in the range [0.023, 0.03], again convergence into a fixed point appears which is now the disease-free equilibrium $E_0 = (200, 0, 0)$. This behaviour is not discussed further but can for example be observed when setting $b = 0.025$.

5.3.2 Initial state 2 – (195.7, 0.03, 3.92)

Trajectories of the second initial state are shown in Fig. 14d–14f. The first interval with similar dynamic behaviour is $b \in [0.01, 0.022)$, where the trajectory **converges** into a **stable fixed point** which is most likely again one of the endemic equilibria (since I & R are non-zero). Again, with rising b the time to convergence rises which is comparable to the behaviour with initial state 1. Fig. 14d shows a relatively low $b = 0.01$ where the system converges fast. For $b > 0.21$ the number of circles before convergence again grows rapidly.
For $b = 0.0219$ the system is still converging to the stable fixed point but no longer linear, similar to initial state 1. Therefore, this value of b is seen as the bifurcation point where the system behaviour changes. A visualisation of this trajectory is given in Fig. 14e.
A different dynamic behaviour is evident for $b \in [0.022, 0.0231)$ where a **stable limit cycle** appears instead of a fixed point. This behaviour is shown in Fig. 14f and is very similar to the simulation for initial state 1. The simulation moves outwards until it converges in the periodic, stable limit cycle. As for initial state 1, the limit cycle is stretched towards the disease-free equilibrium.

Again, convergence to a stable fixed point can be observed for higher $b \in [0.0231, 0.03]$ which is not discussed further here. Similarly to initial state 1, the fixed point seems to be the disease-free equilibrium E_0.

5.3.3 Initial state 3 – (193, 0.08, 6.21)

For initial state 3, the trajectories are visualised in Fig. 14g–14i. As before, the dynamic behaviour is **convergence** to a **stable fixed point** for values of $b \in [0.01, 0.0217)$ where the fixed point is an endemic equilibrium (I & R again non-zero). With rising b the number of circles before convergence/time before convergence rises as seen above for the other initial states. And similarly for $b > 0.021$ this happens especially rapidly. A plot of a trajectory converging to a stable fixed point with $b = 0.015$ can be seen in Fig. 14g.
At $b = 0.0216$ the trajectory is also converging to the fixed point but the convergence is non-exponential and the system is very close to a change in dynamic behaviour. For this reason, $b = 0.0216$ can be seen as the **bifurcation point** and a trajectory very close to the bifurcation point is plotted in Fig. 14h.
Finally, the dynamic behaviour changes for the range of $b \in [0.0217, 0.02203)$ and a **stable limit cycle** appears. Interestingly, for the third initial state the trajectory converges into the periodic behaviour from the outside showing the indeed the limit cycle is stable, which is shown in Fig. 14i for $b = 0.022$.

As before, also the third initial state has a b where it switches back to convergence to a fixed point, i.e. a second bifurcation, which occurs for $b \in [0.02203, 0.03]$. This is not discussed further here, but a nice plot can be obtained for $b = 0.025$ in the Jupyter-notebook.

Figure 14: Trajectories for the three initial states at different values of parameter b plotted in the S-I-plane around $b = 0.022$

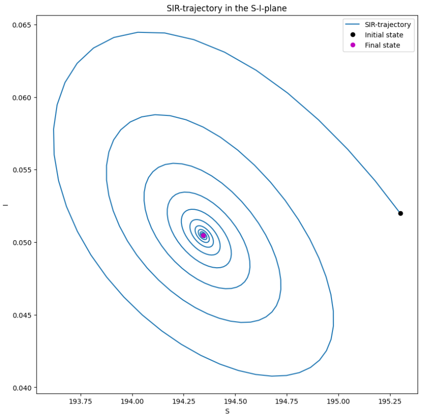

(a) Initial state 1 with b=0.015

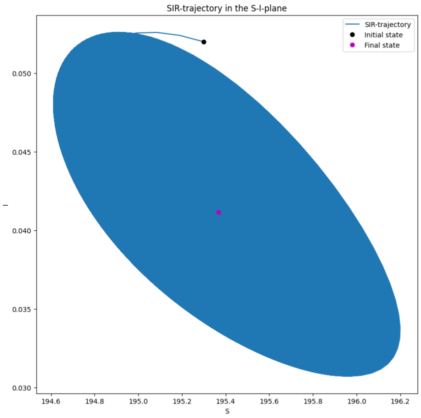

(b) Initial state 1 with b=0.022

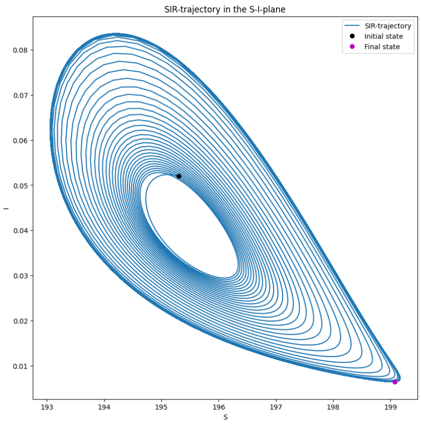

(c) Initial state 1 with b=0.0225

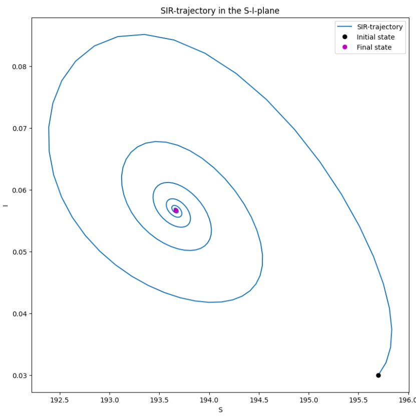

(d) Initial state 2 with b=0.01

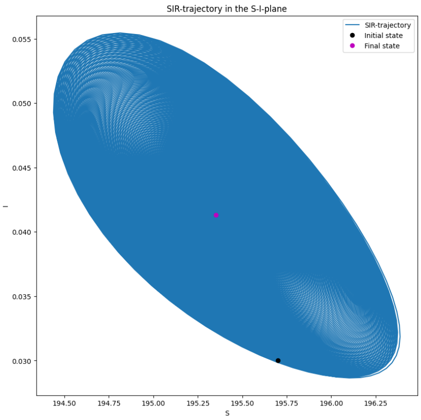

(e) Initial state 2 with b=0.0219

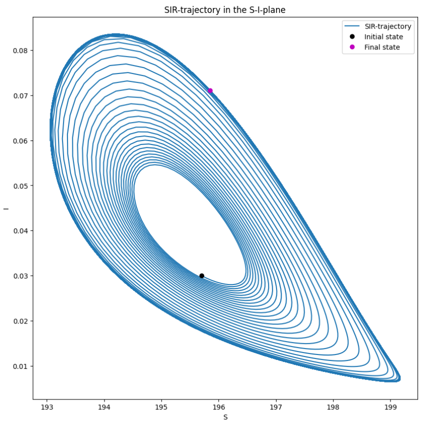

(f) Initial state 2 with b=0.0225

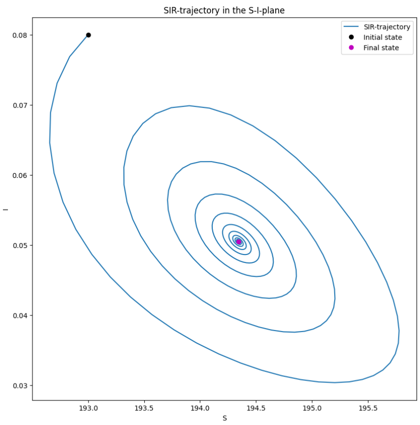

(g) Initial state 3 with b=0.015

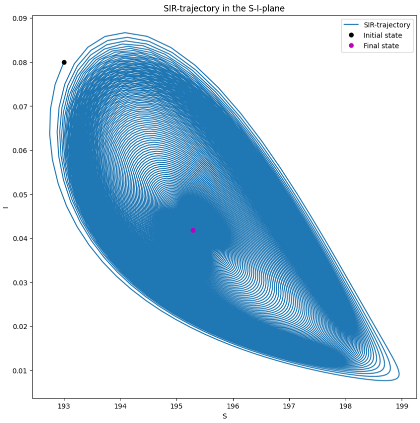

(h) Initial state 3 with b=0.0215

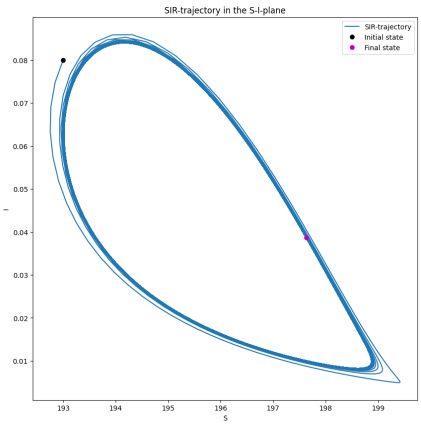

(i) Initial state 3 with b=0.022

5.3.4 Type of bifurcation & normal form

The bifurcation seen in the SIR-model around $b = 0.022$ is a **supercritical Andronov-Hopf-bifurcation** which is evident from the phase diagrams plotted in Fig. 14. Here, we see a change in dynamic behaviour from **convergence into a stable focus**, which is in this case an endemic equilibrium, to the appearance of a **stable limit cycle**. This is exactly the behaviour for an Andronov-Hopf-bifurcation as described in the book by Kuznetsov on page 57 f. and further for the supercritical bifurcation on page 84 ff. [2]. Furthermore, we

see the same behaviour for different initial states with regard to the limit cycle: For states inside the limit cycle (corresponding to low ρ in the book), such as initial state 1 & 2 in the SIR-model, the state converges outwards to the limit cycle due to the gradient being bigger than zero. On the other hand for initial states outside the limit cycle (corresponding to high ρ in the book), such as initial state 3 in our SIR-model, the system approaches the limit cycle from the outside since the gradient is smaller than zero.
The normal form of a supercritical Andronov-Hopf-bifurcation is given in the following. The 2-dimensional normal form holds for the SIR-model since the bifurcation appears on the 2-dimensional center manifold which is proven in the paper by Shan & Zhu [1] on p. 1673 ff.. The normal form was obtained from the book by Kuznetsov [2] on page 84 ff.:
The system in two dimenions x_1 & x_2 can be rewritten in complex form as

$$z = x_1 + ix_2 \tag{6}$$
$$\dot{z} = (\alpha + i)z - z|z|^2 \tag{7}$$

and with the substitution $z = \rho e^{i\varphi}$ we arrive at:

$$\dot{z} = \dot{\rho} e^{i\varphi} + \rho i \dot{\varphi} e^{i\varphi} \tag{8}$$

Subsequently we can specify the polar coordinate normal form of the Hopf-bifurcation as the following:

$$\dot{\rho} = \rho(\alpha - \rho^2) \tag{9}$$
$$\dot{\varphi} = \omega \tag{10}$$

where ω is the angular velocity of the limit cycle which appears if $r > 0$.
The **exact values** for b where the bifurcation happens varies slightly around $b = 0.022$ for the three initial states. The exact values for the appearance of the limit cycle are $b_1 = 0.0221$ for initial state 1, $b_2 = 0.022$ for initial state 2 & $b_3 = 0.0217$ for initial state 3.

5.3.5 Existence of a second bifurcation around $b = 0.023$

Besides the supercritical Hopf-bifurcation occuring in a local neighbourhood of $b = 0.022$, a second Hopf-bifurcation can be found when going to higher b-values, specifically around $b = 0.023$. Here, the dynamic behaviour changes from the stable limit cycle observed for $b > 0.022$ to convergence to a stable focus, namely the disease-free equilibrium $E_0 = (200, 0, 0)$. We will not further discuss this bifurcation here, but plots & the list of final states in the Jupyter notebook show this behaviour. The specific bifurcation points are as follows: $b = 0.023$ for initial state 1, $b = 0.0231$ for initial state 2 & $b = 0.02203$ for initial state 3.

5.4 Reproduction Rate $\mathbb{R}_0$

The formula for the reproduction rate R_0 according to [1] is given in equation (11).

$$\mathbb{R}_0 = \frac{\beta}{d + v + \mu_1} \tag{11}$$

The variables used to describe this reproduction rate $\mathbb{R}_0$ are β, d, v, and μ_1. The variable β is the average number of sufficient contacts with infectious individuals per unit time and d is a value concerning the natural death rate of an individual in the population. v is the disease-induced death rate per person and μ_1 recalls the maximum recovery rate of an individual with $\mu(b, I) = \mu(b, 0) = \mu_1 > 0$.

With $\beta, d, v, \mu_1 > 0$, it holds that the divisor is always a positive number. Therefore, the reproduction rate $\mathbb{R}_0$ is also always greater zero.

Now, let $d, v, \mu_1 > 0$ be fixed. Then the only changing parameter is β and if β is smaller than the value of the divisor in (11) then its reproduction rate $\mathbb{R}_0$ results in a value between 0 and 1. This results in an unchanged number of infectious people since the rate is not high enough to lead to an increase nor low enough to lead to a decrease at a fixed time stamp. However, in the long run, this would lead to a decrease in total number of infected people since there are no new infectious people but the existing ill population can decrease through either natural death or healing process.

In other hand, if β is greater than the sum of d, v, and μ_1 then the reproduction rate $\mathbb{R}_0$ is > 1 and the number of infectious people increases. Since $\beta > 0$ per definition, this reproduction rate (11) can only lead to either an unchanged state or an increased number of infectious people during time. An unchanged state appears when the number of healed (and dead) people cancels out the amount of newly infected people (new infected = healed population). Analogically, an increase in infectious people results from a higher reproduction rate than the healing and dying (from infection) rate combined.

5.5 Attracting node E_0

According to [1], there is an attracting node at equilibrium point E_0 described as followed:

$$E_0 = (A/d, 0, 0) \text{ at } \mathbb{R}_0 < 1 \tag{12}$$

An attracting node, also known as a *stable node*, is a type of equilibrium point where trajectories in its vicinity are drawn towards it as time progresses. Therefore, for the values (S, I, R) close to E_0 the infectious (I) and removed (R) part of the population is drawn towards zero while the susceptible (S) number of people is drawn towards the value of $\frac{A}{d}$. Since A is the birth rate of the susceptible population and d the death rate with $d > 0$, the real value of S is always positive and constant around the stable point E_0.

This means that around the attracting node E_0 the infection as well as the recovery is not spread as the time passes while there are close to $\frac{A}{d}$ many susceptible people. This resolution co-exists with the condition that the reproduction rate of $\mathbb{R}_0 < 1$ results in a behaviour of non-spreading action over time (see explanation above).

References

[1] Chunhua Shan and Huaiping Zhu. Bifurcations and complex dynamics of an SIR model with the impact of the number of hospital beds. *Journal of Differential Equations*, 257(5):1662–1688, September 2014.

[2] Yuri A. Kuznetzov. Elements of Applied Bifurcation Theory. *Springer New York*. 2012.